Overview of 9Cr steels properties for structural application in sodium fast reactors

Laurent Forest, Celine Cabet, Jean-Louis Courouau, France Dalle, L. Martinelli, M. Sauzay

Overview of 9Cr steels properties for structural application in sodium fast reactors

Céline Cabet*, Jean-Louis Courouau, France Dalle, Clara Desgranges, Laurent Forest, Laure Martinelli and Maxime Sauzay

CEA, DEN/DANS
CEA Saclay, France

Abstract

A research and development programme has been launched by CEA, EDF and AREVA for the choice and qualification of material for sodium fast reactor (SFR) structural components. The requirements on steam generator (SG) are demanding, with operating temperatures ranging from 240 °C to 530 °C in water/steam and in sodium for an extended design life of several decades. The selection of the SG materials is based on many characteristics: fabrication, welding, thermal properties, mechanical strength at low and high temperature, environmental resistance. 9%Cr steels which are relevant candidate alloys for different designs of SGs have been extensively studied in the past decade. The objective of this paper is to review some advances made at CEA on determining properties of the X10CrMoVNb9-1 steel (hereafter named "grade 91"): welding, modelling of cyclic softening, modelling of long-term creep, compatibility with liquid sodium, corrosion in steam.

Introduction

Sodium fast reactor (SFR) is considered in France as the most mature Generation IV system and the pre-conceptual design of the SFR prototype ASTRID (Advanced Sodium Technological Reactor for Industrial Demonstration) is underway. Material selection and qualification for the major components of ASTRID is a key point for the reactor design and construction. CEA, EDF and AREVA have launched an R&D programme in support of the material validation. Because of their characteristics at high temperature and superior thermal properties (high thermal conductivity, low thermal expansion), 9%Cr steels were contemplated for different designs of steam generators (SG). The operating conditions of SG are demanding with service temperatures ranging from 240°C to 530°C in liquid sodium and water/steam for long design life (several decades). This places high requirements on 9%Cr steels-base metal and welds in terms of long-term behaviour and end-of-life residual properties.

This paper covers some of the latest CEA developments about welding of "grade 91" which is a critical requirement for the construction of large components. It also reviews some of the recent results gained at CEA on the "grade 91" life time assessment in terms of cyclic softening, modelling of long-term creep and compatibility with liquid sodium and steam.

Welding

"grade 91" has wide applications for heat exchanger in the power generation industry, concerning mainly thin structures optimised for creep considerations. As candidate for structural material of SFR SGs, the compromise between achieving good ductility properties and room/high temperature mechanical resistance in welds is needed, granting at a minimum to fulfill requirements of the Order of 12 December 2005 relative to Nuclear Pressure Equipment Arrêté (AESPN). This is why a parametric study was carried out at CEA on welding conditions to improve the welded joint mechanical properties. Many joints have been elaborated by automatic GTAW process with different commercial filler metals (Table 1) and different welding conditions: pulse or continuous welding current, deposition rate (between 0.20 and 1.89 g/cm), post-weld heat treatment temperature (PWHT between 740˚C and 760˚C). The resulting microstructure, impact test and tensile properties were studied.

Table 1: Chemical composition of tested filler materials (mass. %)

Filler metal	C	Si	Mn	P	S	Cr	Mo	Ni	Al	Nb	V	N	Cu
B	0.109	0.22	0.77	0.006	0.002	9.03	0.98	0.46	-	0.059	0.196	0.041	0.03
C	0.09	0.22	0.51	0.005	0.004	8.89	0.91	0.67	0.010	0.08	0.19	0.05	0.03
D	0.08	0.15	1.00	0.006	0.003	9.12	0.89	0.70	-	0.04	0.18	-	0.03

The type of welding current -pulsed or continuous- has little influence on the welded joint microstructure, Ductile-to-Brittle Transition Temperature (DBTT) and ductility. On the other hand the characteristics significantly depend on the deposition rate of filler metal and on the post-weld heat treatment temperature.

- Effect of the deposition rate

Figure 1 shows the impact energy curves for the filler material B, with a PWHT at 760°C and for three different deposition rates. It can be observed that the smaller is the deposition rate per run, the lower is the DBTT. For the lower deposition rate (0.2 g/cm), the welded zone shows a fine fully reaffected grain microstructure, a lower density of precipitates and a lower hardness.

Figure 1: Influence of deposition rate on the weld zone impact energy of "grade 91" (VWT specimens 55×10×10mm³)

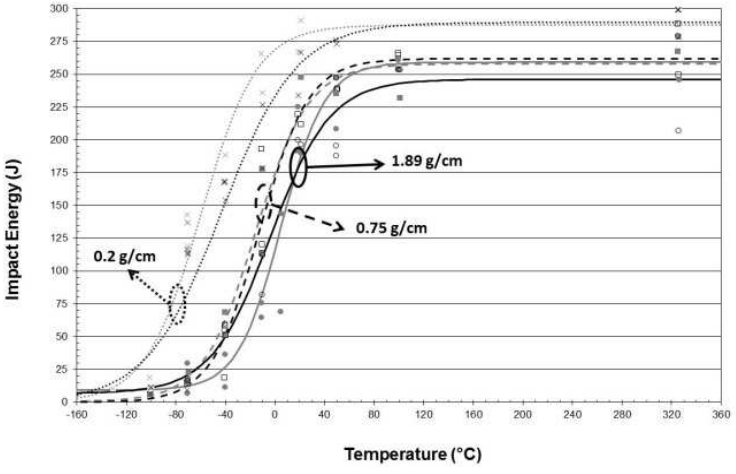

Tensile tests were performed on specimens from the welded zone. While the influence of deposition rate on the tensile strength is insignificant, a decrease in the deposition rate generally causes an increase in the elongation. For instance, filler material B shows an increase in elongation of 7% (PWHT at 740°C) and 12% (PWHT at 760°C) when the deposition rate changes from 1.89 g/cm to 0.2 g/cm.

- Effect of the PWHT

Generally speaking (for filler metal B and C), an increase in the PWHT temperature causes an improvement of elongation after fracture and a diminution of the tensile strength (Rm) at room temperature. The maximum elongation is in decreasing order:

- 25% for product B , PWHT at 760°C, deposition rate 0.75 g/cm;
- 23% for product D, PWHT at 760°C, deposition rate 0.75 g/cm;
- 22% for product C, PWHT at 760°C, deposition rate 0.75 g/cm.

For a PWHT at 740°C, only one tested condition produces Rm below 800 MPa (product D, deposition rate 1.51 g/cm). On the other hand, for a PWHT at 760°C, filler metals B and D exhibit Rm below 800 MPa.

It is concluded that elongation and tensile strength are highly sensitive to the temperature PWHT (740°C-760°C).

Among all tested products and assessed operating conditions, the filler material B with PWHT at 760°C is the most promising with an elongation well higher than 20% and Rm ~580-760 MPa at room temperature.

To complete these mechanical results, it is necessary to check the stability of these properties after ageing treatments. This work is currently in progress on a joint with the identified optimised parameters.

Cyclic softening

The cyclic softening of 9%Cr steels has been extensively studied in the past few years. Alarming results were first obtained on the drop of creep rupture life for pre-cycled specimens with high fatigue damage. Recent data have shown that for more realistic pre-fatigue damage, the creep properties are only moderately impacted. Work is ongoing to quantify the effect of fatigue damage on the creep behaviour. In the meantime, cyclic softening is studied from an experimental and numerical perspective. Recently a micromechanical model has been proposed for predicting both the microstructure evolution and the macroscopic softening of 9%Cr steels [1]. This model based on the self-consistent Kröner homogenisation model [2] is suitable for elastic-plastic constitutive laws. Each martensite block is successively considered as an inclusion within the matrix made of other blocks. The behaviour of the polycrystal is then calculated by an average process over all blocks.

Based on the microstructure evolution as identified through TEM observations [3], two different softening mechanisms are taken into account: the decrease in dislocation densities inside the subgrains and the subgrain size growth. The subgrain size growth is mostly due to the disappearance of low angle boundary dislocations. The final model is mainly based on physical parameters determined from the literature or by microstructural observations and only depends on two adjustable parameters. These two parameters (volume and energy of activation) are fitted from the loading data of the first fatigue loop. The model was applied to 9%Cr steel ''grade 92'' for two different strain rates (Figure 2a). The homogenisation modelling gives good predictions of the cycling softening. It also gives reasonable predictions of the evolution of the subgrain size during cycling with a quick increase at the beginning and then continuous but lower evolution (Figure 2b).

Further work is in progress to take into account other dislocation movements such as climb and to improve the predictions at high temperature. A localisation law adapted from the approach of Molinari et al. [4] will also be implemented to better approximate the viscoplastic behaviour of these steels. With only two fitted parameters, this micromechanical model is an important step forward to predict the real softening of 9%Cr steels in service.

Figure 2: Predictions of the pure fatigue behaviour of "grade 92" for two strain rates

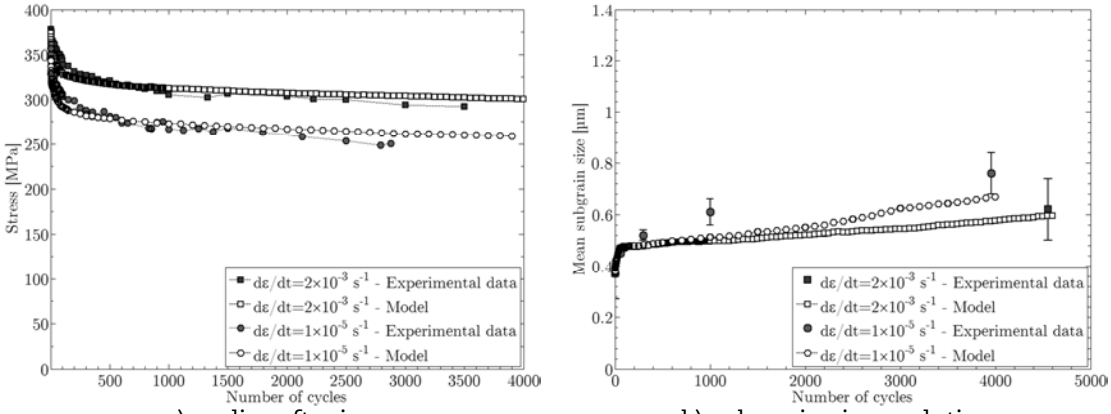

a) cyclic softening b) sub-grain size evolution

Long-term creep damage

Long-term tests have been carried out on 9%Cr steel up to 250 000 h. Observations of failed specimens show that necking is the dominant damage mechanism up to 100 000 h at 600°C and 200 000 h at 500°C [5]. Necking has been simulated taking into account the softening behaviour of martensitic steels; the predicted lifetimes are close to the experimental points (Figure 3a) for:

- a large range of temperatures: 500-700°C,
- a very large range of lifetimes: from one hour to more than 100 000 h,
- all considered martensitic steels whatever the chemical composition and tempering parameters provided the minimum creep strain rates have been measured.

Therefore a master curve is obtained which is in good agreement with experimental data. It should be noticed that even the cross-section evolution during creep tests is well simulated (figure 3b).

Figure 3:
a) Experimental creep lifetimes obtained for various martensitic steels and temperatures (500-700°C) and predicted lifetimes based on necking simulation (upper and lower bounds)
b) Measured and simulated cross-sections for interrupted test on 9%Cr steel at 550°C and 350MPa [6]

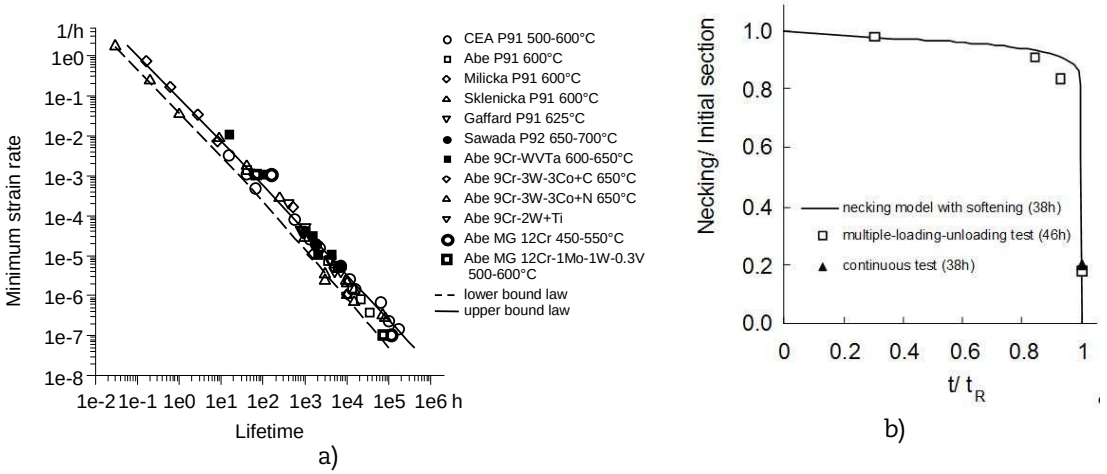

a) b)

For the longest creep tests, intergranular creep cavities are observed (Figure 4a) even if their volume fraction remains very low and do not affect lifetimes up to 100 000 h [6-7].

For longer times, their volume fraction increases and the cavities may affect the lifetime. That is why an additional modelling has been carried out assuming:

- continuous cavity nucleation during creep deformation in agreement with observations;
- cavity growth by vacancy diffusion along grain boundaries which has been shown to be the dominant growth mechanism for martensitic steels in the considered loading conditions.

At 600°C, a change in the stress-time to failure curve is expected. The predicted transition point is about 300 000-400 000 h. This is in good agreement with the only available experimental result at very low stress (70 MPa, 600°C) (Figure 4b).

Figure 4:
a) Intergranular creep cavities in 9%Cr steel tested at 230MPa and 500C for 16 0000 h
b) experimental and predicted lifetime (grey symbols: test data, green line: necking simulation and blue/red curves: intergranular damage simulations) [7]

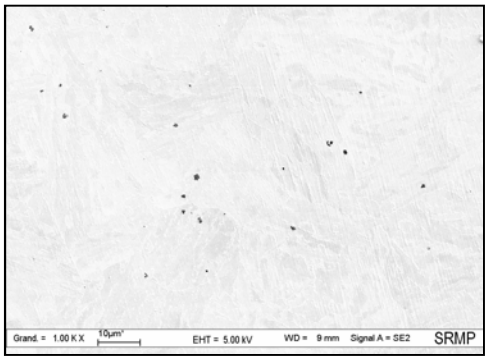

a)

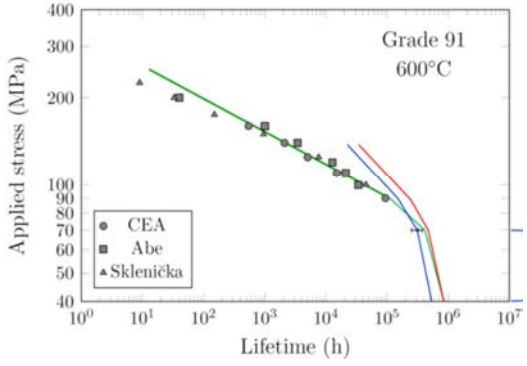

b)

Long-term compatibility with liquid sodium

Few compatibility data are available for 9%Cr steels in sodium at 550°C let alone on the corrosion behaviour on the long run. Therefore, static tests were performed on "grade 91" at 550°C for 1 600 h (test 1) and 5 000 h (test 2) in slightly oxidising and carburising liquid sodium. The oxygen concentration was roughly 10 wppm (µg/g). Samples were extracted every 400 h for test 1 and every 1 000 h for test 2. Characterisation of the corroded specimen morphology includes SEM, XRD, and Glow Discharge-Optical Emission Spectroscopy [8].

Corrosion occurs through oxidation of the sodium-steel interface with the formation of [8-9]:

- a sodium chromite scale ($NaCrO_2$);
- a chromium depleted steel layer where sodium has penetrated (Figure 5a);
- a carburised layer, which is neither hardened nor softened.

The Cr depleted layer exhibits a specific microstructure (martensite tempered laths) and sodium fills the porosity. It is believed that the silicon plays a role in that intergranular attack by promoting the formation of SiO_2 that is then dissolved in sodium through the formation of ($Na_2O.SiO_2$). To our knowledge, this penetration of sodium into the Cr depleted layer has not been documented yet and might play a critical part in the corrosion mechanisms or for other related phenomenon such as liquid metal embrittlement [10]. Further investigations are in progress.

Corrosion kinetics is assessed based on the thickness of each corrosion layer from GD-OES analyses. Both chromium and carbon concentration profiles are used to localise the interfaces between the corrosion layers [8]. This technique appears to be accurate to

evaluate the evolution of the mean thickness over few micrometers even if interfaces are partly inhomogeneous. The thickness of the oxide scale is plotted against time in Figure 5b for both the "grade 91" and the austenitic Stainless Steel 316L(N) (X2CrNiMo17-12-2 controlled nitrogen content) [9]. After 5 000 hours, the oxide scale is 2.5 times thicker than for SS 316L(N), while the Cr depleted layer of "grade 91" steel is 7 times thicker. Thus, "grade 91" appears to be more sensitive to oxidation than austenitic steels andis in agreement with literature data. Both linear and parabolic evolution of the scale thickness fits with the data and results at longer times are needed to discriminate the corrosion law. The rate limiting step of the oxidation mechanism has also to be identified. To complete the experimental database, long-term corrosion tests are ongoing with different oxygen concentration (0 and 200 wppm) at 550°C.

Figure 5: Oxidation of "grade 91" steel in liquid sodium (slightly oxidising and carburising) at 550˚C

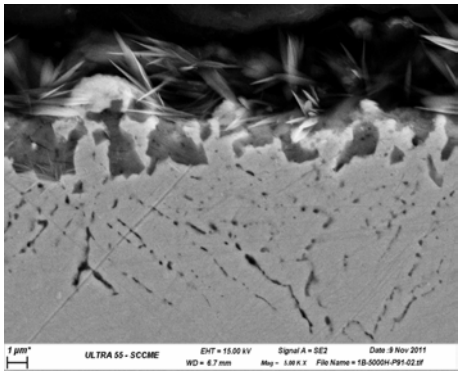

a) specimen exposed for 5 000 h

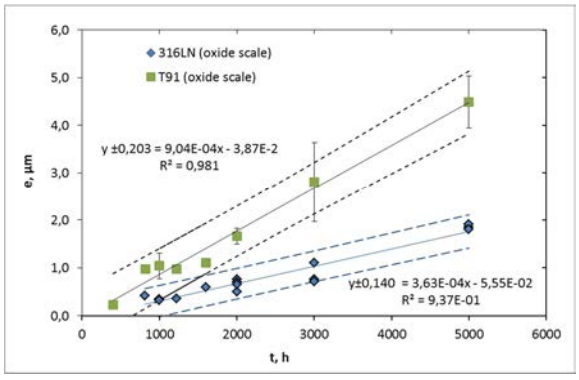

b) evolution of the oxide scale thickness (with 95% confidence hyperboloids) assessed by GD-OES (SS 316LN as reference)

Oxidation in steam

The oxidation of "grade 91" steels in water/steam is an important issue for steam generator applications. The metal loss through oxidation in service must be assessed to design the tube thickness. A dedicated device was developed to perform oxidation experiments in pure water vapour with a circulation loop. The tests were carried out at 550°C and at atmospheric pressure up to 5 000 h. Three sample holders (with two specimens each) were placed in the quartz tube of a furnace and were exposed to pure water vapour with a low flow rate.

Samples were analysed by SEM, Raman spectroscopy and TEM (Figure 6). All samples present the same oxide scale morphology with a three-layer structure consistent with literature data [11]:

- a Fe-Cr spinel layer ($Fe_{3-x}Cr_xO_4$, $0<x<2$) at the metal/oxide interface;
- a magnetite (Fe_3O_4) layer in contact with steam;
- a layer of hematite, formed by oxidation of the magnetite, on top of the magnetite layer.

TEM examinations show that the spinel oxide is composed of a large quantity of small equiaxial grains with an average stoichiometry $Fe_{2.4}Cr_{0.6}O_4$. Near the base metal, Fe-rich and Cr-rich grains are alternatively observed. This observation is in good agreement with the oxidation mechanism proposed to describe the main oxidation process [12]: oxygen is brought to the metal/spinel interface in the molecular form (water molecule). The anionic growth of the internal scale is controlled by the space made available by the metal loss due to formation of the external magnetite scale by cationic flux.

Figure 6: Oxidation of "grade 91" steels in pure steam (holder #3)

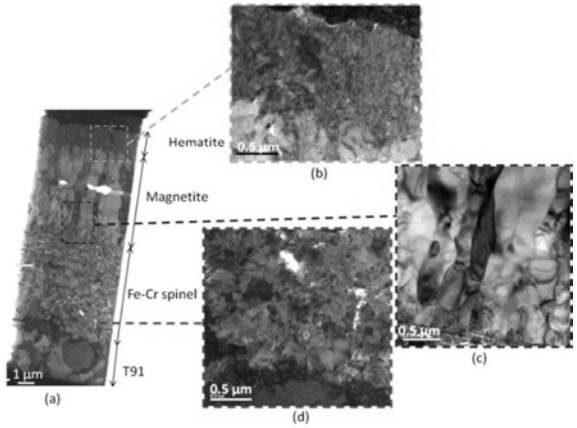

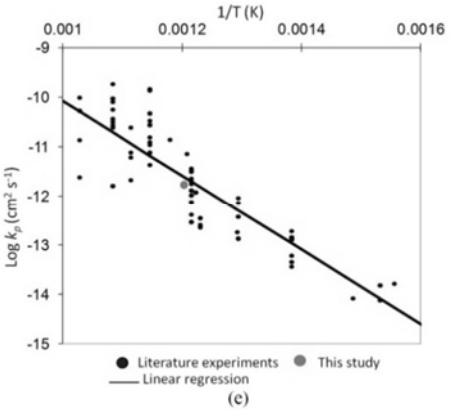

a) TEM picture (48 hours)
b) zoom on the hematite layer
c) zoom on the magnetite layer
d) zoom on the Fe-Cr spinel layer

e) parabolic constants versus temperature

The evolution of the weight gains (from 48 h up to 5 000 h) is shown in Figure 7. The obtained oxidation kinetics is parabolic up to 1 700 h. Figure 7 shows that oxidation rate depends on the sample position in the furnace. In fact, samples from holder #3, which was located downstream of the flow show the higher oxidation rate; and samples from holder #1 placed upstream show the lower oxidation rate. It is believed that the difference in the kinetics with the sample position is linked to the flow rate of water vapour. The reason is not completely understood but it must be linked to the hydrogen production formed during the oxidation of 9%Cr steel by water. The parabolic constant of samples in the downstream position (sample holder #3) is consistent with literature results as observed in Figure 6e.

Figure 7: Oxidation of "grade 91" steel in pure steam: evolution of the mass gain

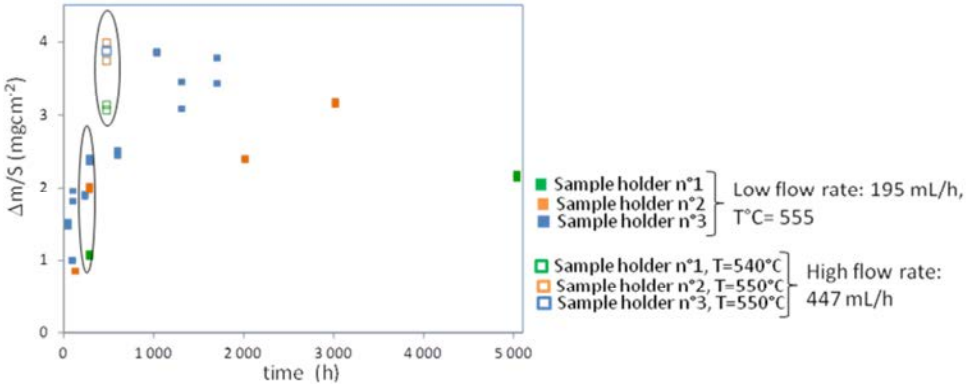

Conclusion

In support of the development of steam generator and circuit for SFR, CEA, EDF and AREVA have extensively studied the properties of 9%Cr steels for several years. Key requirements for "grade 91" steel are the welding of thick components and a design life of 30 years. An overview is given on some recent R&D results obtained at CEA. Development of the welding procedure is ongoing and promising results were obtained through decreasing the quantity of filler metal deposited per run and through improvement of the post-weld heat treatment. For the best conditions and filler metal, suitable impact energy, tensile elongation and Rm were measured and the welded joint meets the standard

requirements with acceptable margin. Cyclic softening during pure fatigue tests has been well predicted by a polycrystalline model. Predictions over longer times should be obtained soon. Creep damage mechanisms have been studied in details showing the influence of necking up to 100 000 h at 600°C and the additional effect of intergranular creep cavitation for longer times. Both mechanisms have been simulated leading to predicted lifetimes in reasonable agreement with experimental data up to a few hundred thousand hours. Corrosion of 9%Cr steel was studied in slightly oxidising and carburising liquid sodium at 550°C. Oxidation was evidenced. The corrosion rate of "grade 91" steel is moderate but higher than the rate for austenitic steels; corrosion kinetics needs to be investigated on longer times. Steam oxidation was investigated in pure steam: over long times, "grade 91" steel form rather thick oxide scales made of spinel, magnetite and hematite. Understanding and modelling of oxidation kinetics is going on.

Acknowledgements

AREVA NP and EDF are greatly acknowledged for their financial support. The authors are grateful to Martine Blat-Yrieix, EDF R&D, Sophie Dubiez-Le Goff, AREVA NP, and Thorsten Marlaud, AREVA NP, for fruitful discussions.

References

[1] Giroux, P.F, F. Dalle, M. Sauzay, C.Caës, B. Fournier, T. Morgeneyer, A.F. Gourgues-Lorenzon (2010), Procedia Engineering, Volume 2, pp. 3984-3993.

[2] Kröner, E. (1961), Acta Metallurgica, Volum 9, pp. 155.

[3] Giordana, M.F., P.F. Giroux, I. Alvarez-Armas, M. Sauzay, A. Armas, T. Kruml (2012), Materials Science and Engineering A, 550, pp. 103-111.

[4] Molinari, A., S. Ahzi, R. Kouddane (1997), Mechanics of Materials, 26, pp. 43-62.

[5] Lim, R., M. Sauzay, A.-F. Gourgues (2011) "Modelling and experimental study of the tertiary creep stage of grade 91 steel", International Journal of Fracture, Volume 169, pp. 213-228.

[6] Lim, R., M. Sauzay, F. Dalle, L. Allais, I. Tournié, P. Bonnaillie, A.-F. Gourgues (2012) "Experimental study and modelling of long-term creep lifetime of modified 9Cr1Mo steels", *Creep 2012*, Kyoto, Japan.

[7] Sauzay, M. (2012), "Déformation et endommagement à haute température des aciers martensitiques revenus. Fatigue, fluage et fatigue-fluage", Techniques de l'ingénieur, M4180, Editions T.I., Paris.

[8] Courouau J.-L., V. Lorentz, M. Tabarant, S. Bosonnet, F. Balbaud-Célérier (2013) "Corrosion by oxidation and carburization in liquid sodium at 550C of austenitic steels for sodium fast reactors", in International Conference on Fast Reactors and Related Fuel Cycles (FR13), March, Paris, France.

[9] Courouau, J.-L. et al (2013) ''Corrosion by oxidation and carburization in liquid sodium at 550C of ferritic martensitic steels for sodium fast reactors'', this conference.

[10] Hemery, S., T. Auger, J.L. Courouau, F. Balbaud-Célérier (2013) ''Effect of oxygen on liquid sodium embrittlement of T91 martensitic steel'', Corrosion Science, doi: http://dx.doi.org/10.1016/j.corsci.

[11] Wright, I.G., R.B. Dooley (2010), International Materials Reviews, 55, 3, pp. 129.

[12] Martinelli, L., F. Balbaud-Célérier, A. Terlain, S. Bosonnet, G. Picard, G. Santarini (2008), Corrision Science, Volume 50, pp. 2537.